J. Phys. Chem. A **1999,** *103,* 3438−3441

Temperature Effects on the Kinetics of Carbonate Radical Reactions in Near-Critical and Supercritical Water

John L. Ferry and Marye Anne Fox*

Department of Chemistry and Biochemistry, University of Texas at Austin, Austin, Texas 78712

Received: November 19, 1998; In Final Form: February 24, 1999

Pulse radiolysis was used to generate the carbonate radical ($CO_3^{-\bullet}$) in subcritical and supercritical water. The effect of the charge of the reaction partner on the kinetics of the reaction with aqueous carbonate radical was examined over the temperature range 30−400 °C, at 4150 ± 75 psia, pH 10.55. The rate constant for oxide transfer between two $CO_3^{-\bullet}$ radicals was insensitive to temperature below 200 °C, but increased by a factor of 300 from 1.61×10^7 to 2.90×10^9 M^{-1} s^{-1} between 200 and 400 °C. The rate constants for the one-electron oxidation of aniline, *p*-aminobenzoate, *N*,*N*-dimethylaniline, and *p*-*N*,*N*-dimethylaminobenzoate by $CO_3^{-\bullet}$ under the same conditions all displayed a negative temperature dependence at temperatures below 320 °C. Above 320 °C, the rate constants for the oxidation of the anionic aminobenzoates by $CO_3^{-\bullet}$ increased sharply, whereas those for the oxidations of the corresponding neutral anilines did not increase until 360 °C.

Introduction

The high solubility of organic compounds and dioxygen in near-critical and supercritical water makes these environments attractive media for both the oxidation of hazardous waste and the controlled synthesis of organic chemicals.[1−3] The dioxygen-mediated mineralization of organic compounds in subcritical and supercritical water ($T_c = 374.2$ °C; $P_c = 3160$ psia) is thought to involve the intermediacy of hydroxyl ($HO^\bullet$) and hydroperoxyl ($HOO^\bullet$) radicals.[4,5] Carbon dioxide produced during mineralization would be converted in water to the resulting carbonic acid ($pK_a = 6.35$) which can be deprotonated to bicarbonate (HCO_3^-) and carbonate anions (CO_3^{2-}).[6,7] These anions both react with hydroxyl radicals to produce carbonate radicals ($CO_3^{-\bullet}$), eqs 1 and 2:[8,9]

$$HO^\bullet + HCO_3^- \xrightarrow{k_1} H_2O + CO_3^{-\bullet} \quad k_1 = 8.50 \times 10^6\ M^{-1}\ s^{-1} \tag{1}$$

$$HO^\bullet + CO_3^{2-} \xrightarrow{k_2} HO^- + CO_3^{-\bullet} \quad k_2 = 3.90 \times 10^8\ M^{-1}\ s^{-1} \tag{2}$$

These equations represent significant competitive reactions for $HO^\bullet$ in such systems, since the total carbonate concentration can be high relative to other scavengers.[10] Although $CO_3^{-\bullet}$ reacts more slowly than $HO^\bullet$ with most organic substrates,[11−13] it is nonetheless a strong oxidant (1.50 V vs the NHE).[11−13] Given its probable significance as an oxidant in the latter stages of mineralization in aerated supercritical water, it is important to understand its kinetic behavior at high temperatures. Previous studies have noted that many bimolecular reactions of $CO_3^{-\bullet}$ exhibit a small or even negative temperature dependence over the temperature range 20−80 °C.[14,15] These observations suggest that $CO_3^{-\bullet}$ may be a sensitive probe of changing water structure on reactions occurring in the compressible region.

As fluids approach their critical point, their dielectric constants change dramatically as a function of temperature and pressure.[1] This means that the same solute will experience a very different local solvation in a near-critical fluid than in the same liquid under standard condition. This altered structure can have a significant effect on partitioning between competing reactions if one pathway has a transition state that is better supported by the near-supercritical fluid than another. One illustration of this effect is the photochemical dimerization of isophorone in supercritical HCF_3 and in supercritical CO_2,[16] where pressure changes produced a change in dielectric, which in turn favored the regiopreference for the polar head-to-head dimer. In a similar vein, the rates of individual reactions with polar transition states are strongly affected by the solvent dielectric.[17] The oxidation of triethylamine by triplet naphthalene or benzhydryl cation are examples of this latter effect.[17,18]

Pulse radiolysis has been used extensively in the study of free radical reactions in near-critical and supercritical aqueous solutions.[19.20] The effect of temperature on hydroxyl radical produced within the radiolysis pulse has been mapped from 20 to 330 °C.[19] Ferry and Fox observed a shift in the mechanism by which $HO^\bullet$ oxidizes phenolate anions as a function of temperature, showing that high temperatures favor one-electron oxidation over addition to the aromatic ring.[20] The experimental apparatus used in these experiments is generally not sufficiently robust to withstand the high temperature, pressure, and corrosiveness of these solutions for extended periods, so the experiments are typically conducted under isobaric conditions while temperature is varied. This can make interpretation of the resulting data somewhat problematic, given that both the solution temperature and the fluid dielectric constant are changing throughout the experiment.

In this study, the rate constants for the oxidation of aromatic amines by $CO_3^{-\bullet}$ are measured over the temperature range 40−400 °C by monitoring the transient absorbance of $CO_3^{-\bullet}$ at 600 nm. The log *k* vs *T* profiles for the oxidation of aniline (AN), *N*,*N*-dimethylaniline (DMAN), *p*-aminobenzoate anion (AB), and *N*,*N*-dimethylaminobenzoate anions (DMAB) by $CO_3^{-\bullet}$ are used to illustrate the effect of the changing structure of water in the near-critical region on the reaction between anionic reactant with a neutral and an anionic substrate.

---

* Current address: Office of Chancellor, North Carolina State University, Raleigh, NC 27695.

10.1021/jp984485d CCC: $18.00

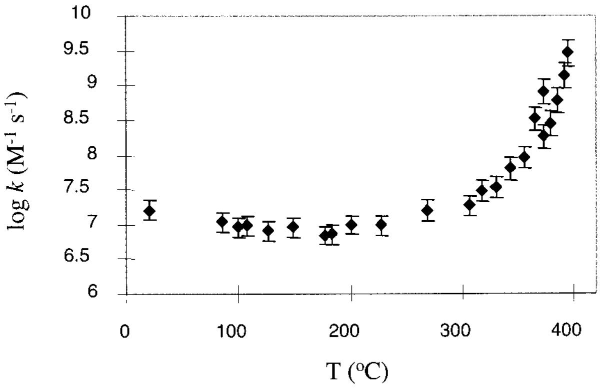

Figure 1. Rate constants for $CO_3^{-\bullet}$ decay as a function of temperature (4150 psia, 9.40 mM K_2CO_3, transient absorbance monitored at 600 nm).

Experimental Section

Materials. AN (99%), DMAN (99%), AB (99+%), DMAB (99%), K_2CO_3 (99%), and KSCN (99%) (Aldrich) were used as received. Water was ASTM grade (≥15.7 MΩ), prepared by Millipore filtration.

Pulse Radiolysis. The pulse radiolysis apparatus and the high pressure−high temperature radiolysis cell have been previously described.[20] Aqueous KSCN (1.60×10^{-2} M) was used for dosimetry. From the known absorbance of $(SCN)_2^{-\bullet}$ at 480 nm ($\epsilon_{480} = 7800\ M^{-1}\ cm^{-1}$),[21] the average yield of $HO^\bullet$ was maintained at 5.35×10^{-6} M per pulse, with a standard deviation of approximately 10%. Pulse energy was monitored continuously with a relative energy monitor.[22] The yield of $CO_3^{-\bullet}$ was found to be constant as a function of temperature under these conditions.

Solution Preparation. Aqueous K_2CO_3 (9.40×10^{-3} M) was spiked with sufficient amine to scavenge >95% of all $CO_3^{-\bullet}$ and to ensure first-order decay of $CO_3^{-\bullet}$, based on the known rate constants for the room temperature reaction between $CO_3^{-\bullet}$ and the amine in question (ca. 3.00×10^{-5} M). [23] These solutions were bubbled gently with N_2O for 25 min prior to and throughout the measurement.

Results and Discussion

Carbonate Radical ($CO_3^{-\bullet}$). Pulse radiolysis was used to generate $HO^\bullet$, which reacted with aqueous K_2CO_3 to produce $CO_3^{-\bullet}$.[8,9] The transient absorbance of $CO_3^{-\bullet}$ was monitored directly at its visible absorption maximum, 600 nm ($\epsilon_{600} = 1860\ M^{-1}\ cm^{-1}$).[8] The initial $[CO_3^{2-}]$ was high enough (9.40 mM) that the reaction between $HO^\bullet$ and $CO_3^{-\bullet}$ was pulse-width limited for all experiments.

Under standard conditions, $CO_3^{-\bullet}$ radical decays through a bimolecular oxide radical transfer process,[24] eq 23, with a rate constant of $1.40 \times 10^7\ M^{-1}\ s^{-1}$.[11,24] This value compares favorably with the rate constant measured in this work, i.e., $1.61 \times 10^7\ M^{-1}\ s^{-1}$ at 21 °C, 4150 psia (assuming an error of approximately 4%, based on noise in the transient signal).

$$CO_3^{-\bullet} + CO_3^{-\bullet} \xrightarrow{k_3} CO_4^{2-} + CO_2 \quad k_3 = 1.40 \times 10^7\ M^{-1}\ s^{-1} \qquad (3)$$

In agreement with previous work suggesting that temperature has either no influence or a slightly negative influence on the rate of this reaction,[25] we observed little change in rate constant below 200 °C (Figure 1). Previous work suggests that the inverse relationship between temperature and the reaction rate constant is due to the presence of an intermediate association complex $[(CO_3^{-\bullet})_2]$, eq 4:[15]

$$CO_3^{-\bullet} + CO_3^{-\bullet} \underset{k_{-a}}{\overset{k_a}{\rightleftarrows}} [(CO_3^{-\bullet})_2] \xrightarrow{k_b} CO_4^{2-} + CO_2 \qquad (4)$$

If k_{-a} is larger than k_b and has a higher activation energy than k_a, then E_a for the process will appear negative.[15] However, above 200 °C the rate constant begins to increase slowly, and between 300 °C and 400 °C it increases by approximately 2 orders of magnitude.

Likely this dramatic change reflects a change in local structure. As the hydrogen-bonding network in near-critical water breaks down, independent studies have shown that dissolved ionic materials experience significant solvent clustering and ion pairing.[26] A picosecond lifetime is typically observed for ordered clusters of solvent molecules about a nonelectrolyte in the compressible region,[16] but the lifetimes of ion pairs or higher order charged aggregates is unknown. If dissolved K_2CO_3 aggregates in near-critical and supercritical water, then the local concentration of reactive $CO_3^{-\bullet}$ radicals could be considerably higher than is indicated by their apparent bulk concentration. This effect would cause an apparent increase in the bimolecular rate constant as a function of temperature. Since the decay of $CO_3^{-\bullet}$ remains second order at all temperatures, a significant change in the mechanism of its decay is unlikely as an alternative explanation for these observations, although that possibility cannot be ruled out definitively by these data.

Aromatic Amines. There are two possible mechanisms for the first step by which $CO_3^{-\bullet}$ may oxidize amines: direct hydrogen atom abstraction or one-electron oxidation to produce a cation radical followed by rapid proton transfer.[27,28]

$$CO_3^{-\bullet} + R_2NH \rightarrow HCO_3^{-} + R_2N\bullet \qquad (5)$$

$$CO_3^{-\bullet} + R_3N \rightarrow CO_3^{2-} + R_3N^{+\bullet} \qquad (6)$$

The significant difference between these two pathways (which are competitive for primary and secondary amines) is in the site of $CO_3^{-\bullet}$ attack: the N−H σ bond (eq 5) or the lone pair on N (eq 6).[28]

In this study, a set of substrate molecules was chosen on the basis of their charge state and one-electron oxidation potential as well as the probable mechanism of their initial oxidation by $CO_3^{-\bullet}$ (electron transfer vs hydrogen abstraction, based on the proposed general mechanisms by which $CO_3^{-\bullet}$ and other one-electron oxidants react with primary and tertiary amines),[27,28] detailed in Table 1. The rate constants for their oxidation by $CO_3^{-\bullet}$, obtained from observing the transient absorbance of $CO_3^{-\bullet}$, are plotted as a function of temperature in Figures 2−5. Pressure was held constant at 4150 ± 75 psia for all experiments.

In the range from room temperature to approximately 320 °C, the rate constants for the oxidation of all four compounds by $CO_3^{-\bullet}$ displayed a negative temperature dependence, consistent with the formation of an intermediate association complex.[15] However, as the critical temperature (374.2 °C) was approached, all substrates exhibit an increase in the observed rate constants for oxidation by radiolytically generated $CO_3^{-\bullet}$. A notable feature of this increase was its threshold temperature: Figures 2−5 reveal that the anionic anilines AB and DMAB experience the onset of this rate increase at significantly lower temperatures than do the neutral anilines AN and DMAN (Table 2). The differentiation between anionic and neutral anilines suggests that the increase is a function of the substrate

TABLE 1: Characteristics of Substrate Amines

substrates	charge[a]	E_{ox} (vs NHE)[13]	bond dissociation energy (kJ/mol)[32]	degree of substitution on N
AN	0	1.030	$H{-}NHC_6H_5$ (368.2 ± 8.4)	1°
DMAN	0	0.770	$H{-}CH_2N(CH_3)C_6H_5$ (352 ± 8)[c]	3°
AB	−1	1.030[b]	$H{-}NHC_6H_5CO_2{-}$(368.2 ± 8.4)[b]	1°
DMAB	−1	0.770[b]	$H{-}CH_2N(CH_3)C_6H_5CO_2{-}$(352 ± 8)[b,c]	3°

[a] At experimental conditions (pH 10.7). [b] Estimation based on the Hammet σ value of p-CO_2^- (0.00).[6] [c] Estimation based on BDE of $H{-}N(CH_3)_2$.[30]

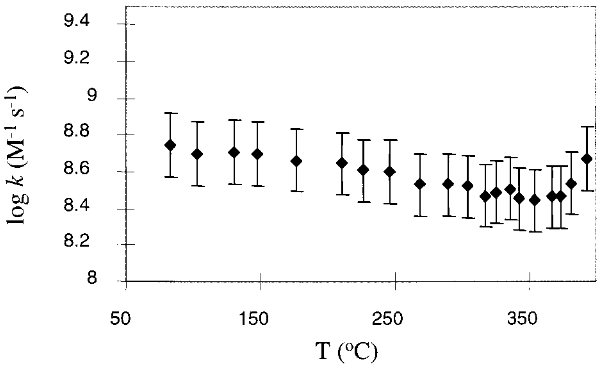

Figure 2. Rate constants for $CO_3^{-\bullet}$ decay as a function of temperature (4150 psia, 9.40 mM K_2CO_3, 33.0 μM AN, transient absorbance monitored at 600 nm).

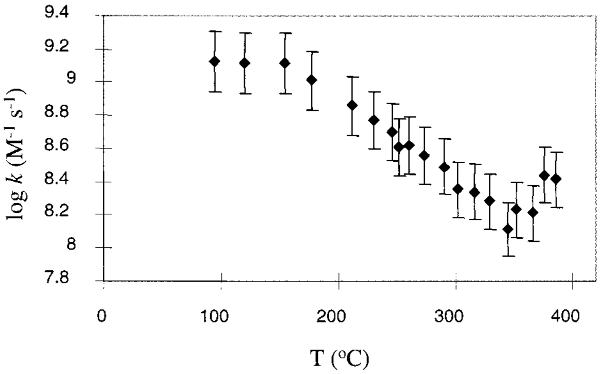

Figure 3. Rate constants for $CO_3^{-\bullet}$ decay as a function of temperature (4150 psia, 9.40 mM K_2CO_3, 41.3 μM DMAN, transient absorbance monitored at 600 nm).

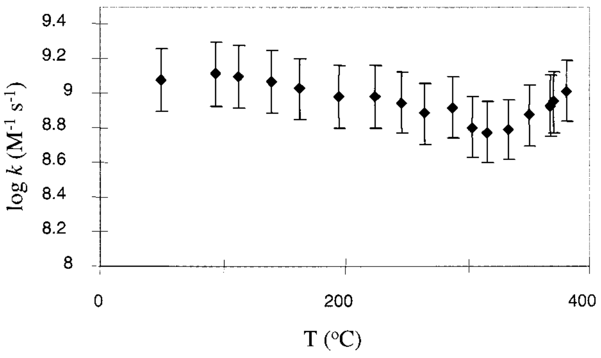

Figure 4. Rate constants for $CO_3^{-\bullet}$ decay as a function of temperature (4150 psia, 9.40 mM K_2CO_3, 27.0 μM AB, transient absorbance monitored at 600 nm).

structure and is not simply inherent to possible artifacts generic to the chemistry of carbonate radicals at high temperature. The fact that the anionic substrates exhibit altered rate profiles at lower temperatures than the neutrals is consistent with enhanced solvent clustering about ions or the formation of aggregates of ion-paired substrates and CO_3^{2-}. The higher local concentration of substrate anions within an aggregate relative to the bulk solution would result in an apparent increase in their rate of oxidation by $CO_3^{-\bullet}$.

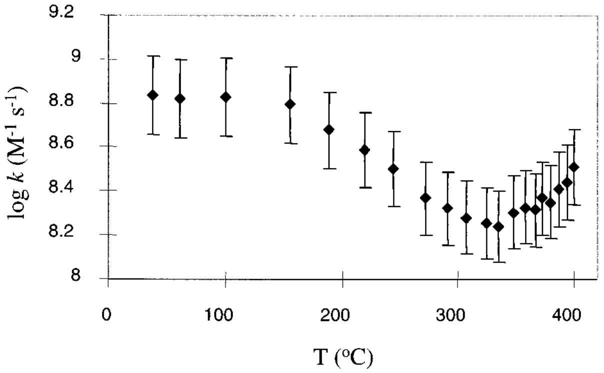

Figure 5. Rate constants for $CO_3^{-\bullet}$ decay as a function of temperature (4150 psia, 9.40 mM K_2CO_3, 39.5 μM DMAB, transient absorbance monitored at 600 nm).

TABLE 2: Onset of Apparent Rate Increase for the Oxidation of All Substrates by $CO_3^{-\bullet}$

substrate	threshold temp (±5 °C)*
AN	360
DMAN	365
AB	315
DMAB	320

[a] From interpolation between minimum rates observed in Figures 2−5.

TABLE 3: Change in Rate Constants for Substrate Oxidation by $CO_3^{-\bullet}$ from Room Temperature to 400 °C

substrate	$(k_{max}/k_{min})^a$
AN	2.00
DMAN	10.3
AB	2.17
DMAB	3.94

[a] For each data set, the factor by which the largest and smallest measured rate constants differ.

Sensitivity to temperature changes also varies with the substrate. Figures 2−5 illustrate that the tertiary amines DMAN and DMAB experience a much larger change in rate constant over the temperature range studied than do the primary amines AN and AB, as shown by the ratio of rate constants k_{max}/k_{min} (the highest rate constant over the lowest) in Table 3. $CO_3^{-\bullet}$ is known to oxidize tertiary amines by direct electron transfer to produce the corresponding cation radical and carbonate anion.[27] Primary amines, however, are often oxidized either by hydrogen abstraction or by electron transfer followed by rapid proton transfer from the relatively acidic N−H bond.[28] In contrast, C−H proton transfer from the α-position of tertiary amines is much slower than N−H proton transfer.[27,28] Thus, the possibility of back electron transfer is increased in the longer-lived encounter complexes produced from the tertiary amines. It is now well-known that the dielectric of liquid water decreases dramatically in the near-critical region.[1] A less polar local environment would likely have little effect on the transition state leading to the neutral amino radical but could significantly destabilize the transition state leading to the amino cation radical. If so, the formation of a more stable polar environment for ion-pair aggregates could contribute to the observed rate enhancements in the temperature range of near-critical water.

Conclusions

The rate constants for the oxidation of primary and tertiary aromatic amines by $CO_3^{-\bullet}$ exhibit significant increases as a function of temperature in near-critical water. The onset temperature of the rate increase is sensitive to the charge on the substrates; the onset for the observed increase in the rate constants for the oxidation of anionic substrates takes place at temperatures lower than for the neutral substrates. This difference is attributed to the increased aggregation of ionic compounds in near-supercritical water relative to neutral compounds.

However, in reactions with polar transition states, such as the oxide radical transfer in the bimolecular decay of $CO_3^{-\bullet}$[24] or an electron transfer during the one-electron oxidation of aromatic amines,[24,28] this aggregation provides a more polar local environment that enhances reactivity and causes an increase in the apparent rate constants. The high ionic strengths developed in near-critical or supercritical water, such as those encountered during the mineralization of concentrated waste streams[29] or in high temperature seawater[30] in oceanic hydrothermal vents, may be able to significantly influence the kinetics of reactions with polar transition states.

Acknowledgment. This work was supported by the National Science Foundation. We express our gratitude to Dr. Don O'Connor and Mr. Bill Naumann of the Center for Fast Kinetics Research for their considerable and patient assistance with the kinetic measurements.

References and Notes

(1) Shaw, R. W.; Brill, T. B.; Clifford, A. A.; Franck, E. U. *Chem. Eng. News* **1991**, *69*, 26.

(2) Sealock, L. J.; Elliott, D. C.; Baker, E. G.; Butner, R. S. *Ind. Eng. Chem. Res.* **1993**, *32*, 1535.

(3) Connolly, J. F. *J. Chem. Eng. Data* **1966**, *11*, 13.

(4) Gopalan, S.; Savage, P. E. *J. Phys. Chem.* **1994**, *98*, 12646.

(5) Crain, N.; Tebbal, S.; Li, L.; Gloyna, E. F. *Ind. Eng. Chem. Res.* **1993**, *32*, 2259.

(6) Gordon, A. J.; Ford, R. A. *The Chemist's Companion*; Wiley-Interscience: New York, 1972; p 137.

(7) Li, R.; Thornton, T. D.; Savage, P. E. *Environ. Sci. Technol.* **1992**, *26*, 2388.

(8) Behar, D.; Czapski, G.; Duchovny, I. *J. Phys. Chem.* **1970**, *74*, 2206.

(9) Buxton, G. V.; Elliot, A. J. *Radiat. Phys. Chem.* **1986**, *27*, 41.

(10) Glaze, W. H.; Kang. J. W.; Chapin, D. H. *Ozone Sci. Eng.* **1987**, *9*, 335.

(11) Buxton, G. V.; Greenstock, C. L.; Helman, W. P.; Ross, A. B. *J. Phys. Chem. Ref. Data* **1988**, *17*, 513.

(12) Wardman, P. *J. Phys. Chem. Ref. Data* **1989**, *18*, 1638.

(13) Neta, P.; Huie, R. E.; Ross, A. B. *J. Phys. Chem. Ref. Data* **1988**, *17*, 1027.

(14) Clifton, C. L.; Huie, R. E. *Int. J. Chem. Kinet.* **1993**, *25*, 199.

(15) Huie, R. E.; Shoute, L. C. T.; Neta, P. *Int. J. Chem. Kinet.* **1991**, *23*, 541.

(16) Hrnjez, B. J.; Mehta, A. J.; Fox, M. A.; Johnston, K. P. *J. Am. Chem. Soc.* **1989**, *111*, 2662.

(17) Brennecke, J. F. In *Supercritical Fluid Engineering Science, Fundamentals and Applications*; Kiran, E., Brennecke, J. F., Eds.; American Chemical Society: Washington, DC, 1993; p 201.

(18) Brennecke, J. F.; Tomasko, D. L.; Eckert, C. A. *J. Phys. Chem.* **1990**, *94*, 7692.

(19) Swiatla-Wojcik, D.; Buxton, G. V. *J. Phys. Chem.* **1995**, *99*, 11464.

(20) Ferry, J. L.; Fox, M. A. *J. Phys. Chem. A* **1998**, *102*, 3705.

(21) Spinks, J. W. T.; Woods, R. J. *An Introduction to Radiation Chemistry*; Wiley-Interscience: New York, 1990.

(22) Fahrataziz, M. A.; Rodgers. *Radiation Chemistry, Principles and Applications*; VCH Publishers: New York, 1987.

(23) Mallard, W. G.; Ross, A. B.; Helman, W. P. *NIST Standard Reference Database 40, NDRL/NIST Solutions Kinetics Database, Version 1.0*; Department of Commerce: Washington, DC, 1992.

(24) Lilie, J.; Hanrahan, J.; Henglein, A. *Radiat. Phys. Chem.* **1978**, *11*, 225.

(25) Eriksen, T. E.; Lind, J.; Merenyi, G. *Radiat. Phys. Chem.***1985**, *26*, 197.

(26) Johnston, K. P.; Balbuena, P. B.; Xiang, T.; Rossky, P. J. In *Innovations in Supercritical Fluids, Science and Technology*, Hutcheson, K. W., Foster, N. R., Eds.; American Chemical Society: Washington, DC, 1996; p 77.

(27) Elango, T. P.; Ramakrishnan, V.; Vancheesan, S.; Kuriacose, J. C. *Tetrahedron* **1985**, *41*, 3837.

(28) Chow, Y. L. *Reactive Intermediates* **1980**, *1*, 151.

(29) Dell'Orco, P. C.; Gloyna, E. F.; Buelow, S. In *Supercritical Fluid Engineering Science, Fundamentals and Applications*; Kiran, E., Brennecke, J. F., Eds.; American Chemical Society: Washington, DC, 1993; p 314.

(30) Stumm, W.; Morgan, J. J. *Aquatic Chemistry, An Introduction Emphasizing Chemical Equilibria in Natural Waters*, 2nd ed.; Wiley-Interscience: New York, 1981.

(31) *CRC Handbook of Chemistry and Physics*; Weast, R. C., Astle, M. J., Beyer, W. H., Eds.; CRC Press: Boca Raton, FL, 1988; p F-179.